antioxidants

MDPI

Article

Copper-Sensitive Metabolic Stress in IL-1β-Induced Dysfunction of Tendon Progenitor Cells: An In Vitro and Transcriptomic Study

Mohammed Zayed [1,2,3], Hadeer Khaled [4], Hilal Tayara [5,*] and Byung-Hoon Jeong [1,2,*]

[1] Korea Zoonosis Research Institute, Jeonbuk National University, Iksan 54531, Republic of Korea; mzayed2@vet.svu.edu.eg
[2] Department of Bioactive Material Sciences, Jeonbuk National University, Jeonju 54896, Republic of Korea
[3] Department of Surgery, College of Veterinary Medicine, Qena University, Qena 83523, Egypt
[4] Laboratory of Veterinary Pathology, College of Veterinary Medicine, Jeonbuk National University, Iksan 54596, Republic of Korea; hadeerekhaled@gmail.com
[5] School of International Engineering and Science, Jeonbuk National University, Jeonju 54896, Republic of Korea
* Correspondence: hilaltayara@jbnu.ac.kr (H.T.); bhjeong@jbnu.ac.kr (B.-H.J.)

Abstract

Tendinopathy is a complex disorder involving inflammation, oxidative stress, extracellular matrix damage, and changes in cellular metabolism. Cuproptosis is a type of regulated cell death that depends on copper and is associated with mitochondrial protein lipoylation and proteotoxic stress. This study investigated whether IL-1β-induced dysfunction of tendon progenitor cells (TPCs) is accompanied by changes in cuproptosis-associated genes and whether pharmacological modulation of copper availability alters this phenotype. Rat TPCs were stimulated with IL-1β, exposed to copper chloride ($CuCl_2$) and the copper ionophore elesclomol (ES), and cotreated with the copper chelator tetrathiomolybdate (TTM). Cellular metabolic activity, gene expression, and reactive oxygen species (ROS) production were assessed. Bulk RNA-sequencing data from IL-1β-treated rat TPCs (GSE253913) and single-cell RNA-sequencing data from cultured human tendon-derived progenitor cells (GSE150482) were analyzed. In rats, transcriptomic analysis showed mainly an inflammatory response to IL-1β, with only slight changes in genes associated with copper and mitochondrial functions. IL-1β decreased TPC metabolic activity and the expression of tenogenic markers such as *Scx*, *Col1a1*, and *Col3a1*, while it increased inflammatory and catabolic markers, ROS production, and the expression of *Dld* and *Lipt1*. TTM attenuated these effects, restoring metabolic activity and some tenogenic markers, and reducing ROS, *Dld*, and *Lipt1* levels. Exposure to ES + Cu triggered a TTM-sensitive phenotype characterized by reduced metabolic activity, decreased expression of tenogenic genes, increased ROS levels, and altered expression of cuproptosis-related genes. The human single-cell dataset analysis also revealed condition-dependent changes in mitochondrial lipoylation genes, including DLAT and DLST. Overall, these findings suggest that inflammatory TPC dysfunction is linked to copper-sensitive mitochondrial stress and gene changes related to cuproptosis pathways.

Keywords: tendinopathy; tendon progenitor cells; copper-sensitive stress; mitochondrial metabolism; inflammation; oxidative stress; cuproptosis-associated genes

Check for updates

Academic Editor: María Candelaria Martín-González

Received: 17 September 2026
Revised: 13 October 2026
Accepted: 16 October 2026
Published: 22 October 2026

Copyright: © 2026 by the authors. Licensee MDPI, Basel, Switzerland. This article is an open access article distributed under the terms and conditions of the Creative Commons Attribution (CC BY) license.

1. Introduction

Tendinopathy commonly affects athletes and non-athletes, often resulting from repetitive mechanical stress or overuse. It can significantly impair the quality of life and physical function of patients [1]. Tendinopathy accounts for approximately 30% of referrals to musculoskeletal physicians [2]. Its pathogenesis is multifactorial and involves repetitive mechanical loading, extracellular matrix (ECM) disruption, inflammation, oxidative stress, cellular dysfunction, and impaired tissue repair. Current conservative treatments, including rest, physiotherapy, and medication, can relieve symptoms [3–6]. Surgical options often lead to disappointing results, with higher rates of complications, including adhesions and tendon rupture [7]. Cell-based therapies have demonstrated potential applications in treating musculoskeletal diseases due to their ability to self-proliferate, differentiate, immunomodulate, and regenerate tissue [8–10]. However, aging, senescence, and inflammation pose challenges for these therapies [11,12]. A better understanding of the cellular and metabolic responses that impair tendon maintenance and regeneration is therefore required.

Tendon progenitor cells (TPCs) contribute to tendon homeostasis and repair through their proliferative and tenogenic capacities. However, inflammatory and oxidative microenvironments can compromise their viability, differentiation, and matrix-producing functions [13–15]. Pro-inflammatory cytokines such as interleukin-1β (IL-1β) can suppress the tenogenic phenotype, increase catabolic activity, and promote oxidative stress in tendon-derived cells [16]. Although IL-1β stimulation does not reproduce all mechanical, structural, and multicellular aspects of tendinopathy, it provides a controlled in vitro model of inflammatory TPC dysfunction relevant to the disease environment. In tendinopathy, oxidative stress and inflammation are closely linked to its progression [17–19]. ROS-driven inflammatory cytokines contribute to ECM degradation, cellular apoptosis, and impaired healing processes [20]. Clinical data support this link; for instance, Abate et al. demonstrated that athletes with tendon damage exhibit higher levels of oxidative stress than those with healthy tendons, highlighting the role of ROS in tendon injury and emphasizing oxidative stress as a key factor in tendon pathology [21].

Copper is an essential trace element that supports mitochondrial respiration, antioxidant defense, iron metabolism, and multiple enzymatic reactions [22]. As a cofactor for enzymes, copper is involved in functions such as mitochondrial respiration, antioxidant defense, and iron metabolism [22,23]. Copper also acts as a dynamic signaling element, affecting lipolysis, cytotoxicity, cell proliferation, and oxidative stress [24]. In this regard, maintaining copper homeostasis is important for cell survival and metabolism [25]. Dysfunctional copper metabolism or regulatory pathways can disrupt copper homeostasis, leading to various diseases, including neurodegenerative disorders, metabolic syndrome, and musculoskeletal and inflammatory conditions [25–27]. It has been reported that copper toxicity disrupts mitochondrial metabolic enzymes, thereby inducing a regulated form of cell death, defined as cuproptosis [28]. Cuproptosis occurs when excess copper binds directly to lipoylated elements of the TCA cycle, leading to proteotoxic stress, mitochondrial damage, and a significant increase in ROS production [27,28]. However, genes identified as related to cuproptosis also play roles in broader processes, including mitochondrial metabolism, protein lipoylation, oxidative stress responses, and copper transport. Variations in these genes or in ROS production suggest pathway involvement or cell susceptibility, but they do not serve as direct, specific indicators of cuproptosis.

The relationship between inflammatory TPC dysfunction and copper-related mitochondrial stress remains underexplored. Since inflammation can impact redox balance and mitochondrial function, we proposed that IL-1β exposure might alter cuproptosis-related metabolic genes and enhance TPC sensitivity to copper-induced stress. We then

investigated how IL-1β, pharmacological ES + Cu stress, and copper chelation with TTM affect TPC metabolic activity, gene expression related to tenogenesis and inflammation, transcripts associated with cuproptosis, and ROS production. Additional analysis of bulk rat and human single-cell transcriptomic datasets was performed to assess if similar transcriptional changes could be observed across different inflammatory and mechanically stimulated TPC models.

2. Materials and Methods

2.1. Study Design and Analytical Framework

The study integrated transcriptomic discovery with targeted in vitro analysis. Rat bulk RNA-sequencing data were first analyzed to characterize the global response of TPCs to IL-1β. Primary rat TPC experiments were then used to evaluate inflammatory, oxidative, tenogenic, and copper-sensitive responses. Human single-cell RNA-sequencing data were analyzed as cross-species contextual evidence in response to mechanical stimulation.

2.2. Transcriptomic Data Sources and Curated Gene Set

Publicly available transcriptomic datasets were obtained from the Gene Expression Omnibus (accessed on 11 March 2026). GSE253913 contains bulk RNA-sequencing data from rat TPCs exposed to IL-1β (50 ng/mL) and was used to assess the broader inflammatory transcriptional response and the expression of selected genes associated with cuproptosis. GSE150482 includes single-cell transcriptomics data from cultured human patellar tendon progenitor cells, collected from three donors per condition and assessed under the specified experimental parameters, including mechanical stimulation [29]. This dataset was utilized to investigate whether mechanical stress influences transcriptional changes in copper transport, mitochondrial metabolism, and protein lipoylation pathways in human tendon cells. A curated list of genes associated with cuproptosis, copper homeostasis, mitochondrial lipoylation, or copper-dependent stress was assembled from published research (see Supplementary Data, Table S1) [28,30,31]. Since many genes on this list are involved in general metabolic and stress-response pathways, the term "cuproptosis-associated genes" was chosen over "cuproptosis markers".

2.3. Rat Bulk RNA-Seq Analysis

Gene expression analysis of RNA-seq data from IL-1β-treated rat TPCs in vitro (GSE253913) was conducted using the limma package (version 3.64.3) in R. FPKM (Fragments Per Kilobase of transcript per Million mapped reads). Values were filtered to remove low-abundance transcripts; only genes with FPKM > 1 in at least three samples were retained for analysis. The filtered data were then log2-transformed with a pseudocount of 1 (log2(FPKM + 1)) to stabilize variance. Differential expression was assessed by fitting a linear model to the log-transformed data. Empirical Bayes moderation was applied to stabilize gene-wise variance estimates. Comparisons were performed between IL-1β-treated and control samples (n = 3 per group). Benjamini–Hochberg correction was applied to account for multiple testing.

2.4. Gene Set Enrichment Analysis

To characterize coordinated transcriptomic changes without limiting the analysis to genes that meet an arbitrary differential-expression cutoff, gene set enrichment analysis (GSEA) was conducted using the full ranked gene list from the comparison between IL-1β-treated and control rat TPCs. Genes were ranked by the moderated t-statistic from limma, with positive values indicating higher expression in IL-1β-treated cells and negative values indicating higher expression in controls. Pathway-level enrichment was assessed

using KEGG pathways and GO: BP gene sets specific to Rattus norvegicus. KEGG and GO: BP GSEA were performed using the gseKEGG and gseGO functions, respectively, in the clusterProfiler package (version 4.16.0). p values were adjusted for multiple testing using the Benjamini–Hochberg procedure, with gene sets with an adjusted $p < 0.05$ considered significantly enriched. The enrichment direction was identified using the normalized enrichment score (NES). A positive NES signified enrichment towards the IL-1β-treated end of the gene list, while a negative NES indicated enrichment in control cells and suppression after IL-1β treatment. Running-enrichment plots were created for specific pathways, and leading-edge genes were defined as those contributing most significantly to the enrichment signal.

2.5. Rat TPC Isolation and Culture

Sprague–Dawley (SD) rats (n = 3, aged 8 weeks, weighing 250 g) were used in this study. The animals were maintained under standard pathogen-free conditions with free access to food and water. All procedures were approved by the Animal Care Committee of Jeonbuk National University (NON2024-093) and performed in accordance with the applicable institutional guidelines. Rats were euthanized by exposing them to an overdose of isoflurane (5%) in an induction chamber. After confirming deep anesthesia through the absence of the pedal withdrawal reflex, euthanasia was completed with cervical dislocation. After euthanasia, the Achilles tendons were harvested from the hind limbs of each rat. The tendon sheath and surrounding paratenon were removed, and the mid-substance of each tendon was minced and digested in phosphate-buffered saline containing 3 mg/mL collagenase type I (FUJIFILM Wako Pure Chemical Corporation, Tokyo, Japan), as previously described [32–34]. The resulting cell suspensions were filtered through a 70 μm cell strainer (BD Falcon, Franklin Lakes, NJ, USA) to obtain a single-cell suspension. The isolated cells were washed by centrifugation in PBS at 1200 rpm for 5 min. They were then resuspended in Dulbecco's Modified Eagle's Medium (DMEM, Gibco, Grand Island, NY, USA) supplemented with 10% fetal bovine serum (Gibco), 100 U/mL penicillin, 100 μg/mL streptomycin, and 2 mM L-glutamine (Gibco) and cultured at 37 °C in an atmosphere of 5% CO_2.

2.6. Cellular Metabolic Activity Assay

TPCs at passage 2–3 were prepared as a cell suspension at a concentration of 2×10^5 cells/mL. A 200 μL aliquot of this suspension was added to each well of a 96-well plate. After adherence, cells were treated with IL-1β (50 ng/mL) for 24 h, in the presence or absence of tetrathiomolybdate (TTM; 20 μm; HY-W076067, MedChemExpress, Monmouth Junction, NJ, USA). To assess TPC responses to pharmacologically induced copper stress, cells were treated with $CuCl_2$ (5–20 μm; C3279, Sigma-Aldrich, St. Louis, MO, USA) and the copper ionophore elesclomol (ES; 50 nm; HY-12040, MedChemExpress) for 24 h, in the presence or absence of TTM. After treatment, the medium was replaced with fresh medium containing 10% CCK-8 reagent. Cells were incubated at 37 °C for 2 h, and absorbance was measured at 450 nm using a microplate reader (Molecular Devices). Because the CCK-8 assay measures cellular reductive/metabolic activity rather than cell death directly, the results were interpreted as changes in cellular metabolic activity.

2.7. RNA Extraction and Quantitative Reverse-Transcription PCR

TPCs were cultured in serum-supplemented DMEM with the indicated treatments, then washed twice with 1× PBS. Total RNA was extracted from the cells using TRIzol reagent (Invitrogen, Waltham, MA, USA) according to the manufacturer's protocol. RNA was reverse-transcribed into complementary DNA, which was analyzed by quantitative reverse-transcription PCR using SYBR Green Master Mix and a CFX96 Real-Time PCR

Detection System (Bio-Rad, Hercules, CA, USA). The expression of the tenogenic and matrix-associated genes *Scx*, *Col1a1*, and *Col3a1*, and the inflammatory and catabolic genes *Il6*, *Mmp3*, and *Mmp13* was evaluated. The expression of selected cuproptosis-associated genes, including *Dld*, *Lipt1*, *Mtf1*, and *Cdkn2a*, was also measured. These genes were evaluated as components of copper-responsive, mitochondrial-metabolic, or cuproptosis-associated processes. Primer sequences are provided in Table 1. Gene expression data were normalized to *Gapdh* and analyzed using the $^{2-\Delta\Delta}$Ct method.

Table 1. List of primers used in quantitative reverse transcription polymerase chain reaction.

Primer	Forward	Reverse
Scx	TGGCCTCCAGCTACATTTCT	TGTCACGGTCTTTGCTCAAC
Col1a1	GCCAAGAAGACATCCCTGAA	GCAGAAAGGACAGCACTCGC
Col3a1	TGATGGGATCCAATGAGGGAGA	GAGTCTCATGGCCTTGCGTGTTT
Il6	AGCGATGATGCACTGTCAGA	GGAACTCCAGAAGACCAGAGC
Mmp3	CAGGCATTGGCACAAAGGTG	GTGGGTCACTTTCCCTGCAT
Mmp13	GCAAACCCTGCGTATTTCCAT	GATAACCATCCGAGCGACCTTT
Dld	AGAGTCTGCCATGCACATCC	ATGTCGAATCTCGTAGACCGT
Lipt1	TCAGCACAAGGTCCCAACAG	CCGATGACGACAGAAGGAGAAT
Mtf1	CATGAAAGGTCACGATAACAAAGG	GGCCCAACTCACTCAGATAAA
Cdkn2a	GCGTTGCCAGAAGTGAAGCCA	CGTCGTGCGGTATTTGCGGTAT
Gapdh	GATGCTGGTGCTGAGTATGACG	GTGGTGCAGGATGCATTGCTCTGA

2.8. Assessment of Intracellular ROS

Intracellular ROS levels were measured using H2DCF-DA (D399, Invitrogen). H2DCF-DA (10 µm) was added to phenol red-free DMEM, and the cells were incubated for 30 min at 37 °C. After incubation, the cells were washed with PBS and imaged using an Olympus IX53 inverted fluorescence microscope (Olympus, Tokyo, Japan) connected to an Olympus DP73 camera (Olympus, Tokyo, Japan). Fluorescence intensity was quantified using ImageJ software version 1.54 (https://imagej.net/ij/). H_2DCF-DA fluorescence was interpreted as a general indicator of intracellular oxidative activity and not as a cuproptosis-specific readout. Three independent experiments were performed.

2.9. Human Single-Cell RNA-Seq and Pseudobulk Analysis

For GSE150482, single-cell count matrices were processed using Scanpy (version 1.11.1) in Python (version 3.12). Gene identifiers were mapped using Ensembl annotations, and cell barcodes were matched to sample-hashing information. Only high-confidence singlets were retained. Quality-control metrics were calculated before data integration. Samples were integrated using single-cell Variational Inference (scVI) via the Virtual Cell Models platform (https://virtualcellmodels.cziscience.com/). scVI integration was used to correct for batch effects across samples while preserving biologically meaningful variation between conditions. The integrated dataset underwent standard downstream processing. A k-nearest neighbor graph was constructed from the scVI latent space (X_scvi). Uniform Manifold Approximation and Projection (UMAP) was then applied to the scVI embeddings to visualize cellular relationships in two dimensions. Cell clusters were identified using the Leiden algorithm with a resolution parameter of 0.5. To maintain the biological replicate structure, differential expression analysis was performed using donor-level pseudobulk profiles rather than treating individual cells as separate replicates. Pseudobulk counts were analyzed with PyDESeq2 (version 0.4.12), using three biological donors per condition.

Single-cell dot plots and UMAPs served as visual tools to illustrate cellular expression patterns. Cuproptosis-associated expression patterns were interpreted as evidence of transcriptional pathway remodeling.

2.10. Statistical Analysis

Statistical analyses of experimental data were performed using GraphPad Prism (version 8.0.2). Data are presented as mean ± standard deviation (SD). Data distribution was assessed to determine the appropriate statistical test. An unpaired Student's *t*-test was used for two-group comparisons, while a one-way ANOVA followed by Tukey's post hoc test was used for multiple-group comparisons. A p-value < 0.05 was considered statistically significant.

For transcriptomic analysis, multiple-testing correction was performed using the Benjamini–Hochberg method. Bioinformatics data processing and analysis were conducted using the R programming environment (version 4.5.2). Differential expression analysis was performed to identify differentially expressed genes (DEGs), with significance defined as an adjusted p-value (Padj) < 0.05 and an absolute log2 fold change ($|\log2FC|$) > 1. Functional enrichment analyses were performed using the clusterProfiler package (version 4.16.0). Gene Ontology (GO) terms and Kyoto Encyclopedia of Genes and Genomes (KEGG) pathways were analyzed to elucidate biological functions. Cuproptosis-associated genes with adjusted p < 0.05 that did not meet the prespecified fold-change threshold were reported as modestly altered genes and were not classified as genome-wide DEGs.

3. Results

3.1. IL-1β Induces an Inflammatory Transcriptomic Response, with Modest Changes in Cuproptosis-Related Genes

We first analyzed the rat bulk RNA-sequencing dataset GSE253913 to define the global transcriptional response of TPCs to IL-1β and determine whether genes associated with copper homeostasis, mitochondrial lipoylation, or cuproptosis were altered within this response. Comparison of IL-1β-treated and control samples identified 678 DEGs, including 480 upregulated and 198 downregulated, indicating substantial transcriptomic remodeling. Unsupervised hierarchical clustering and heatmap analysis confirmed a clear divergence in gene expression profiles, driven primarily by robust upregulation of inflammatory mediators in the IL-1β-treated samples, including Ptx3, Ntn1, Ccl2, Ccl7, Ccl20, and Cxcl3. The expression patterns of these DEGs are shown in the heatmap and volcano plot (Figure 1A,B).

We next evaluated a predefined set of genes associated with copper transport, mitochondrial lipoylation, and cuproptosis. None of these genes met the combined adjusted-p-value and absolute fold-change criteria used to define genome-wide DEGs. However, *Dld*, Gcsh, and Slc31a1 showed statistically significant but modest changes when evaluated using adjusted p < 0.05 in response to IL-1β (Figure 1C). These results indicate limited transcriptional modulation of selected cuproptosis-associated genes rather than broad activation of a cuproptosis program. Although selected copper- and mitochondrial metabolism-associated genes were moderately altered, the transcriptomic data do not establish endogenous copper accumulation or increased susceptibility to copper toxicity. Complementary GO enrichment (Biological Processes) further identified responses to IL-1, bacterial products, lipopolysaccharide, and chemotactic signals (Figure 1D) [35]. To elucidate the mechanisms driving this sensitivity, we performed functional enrichment analysis on the global DEGs to display pathway significance and enrichment magnitude. KEGG pathway analysis revealed that the DEGs were heavily enriched in signaling cascades associated with inflammation, with the strongest enrichment observed in the TNF signaling

pathway, IL-17 signaling pathway, and NF-κB signaling pathway [36–39], and cytokine–cytokine receptor interaction (Figure 1E) [40]. These pathways indicate a pronounced inflammatory and stress-response profile, but they are not unique to cuproptosis. Taken together, results suggest that IL-1β promotes an inflammatory, metabolically disrupted cellular environment, potentially altering copper-related stress responses.

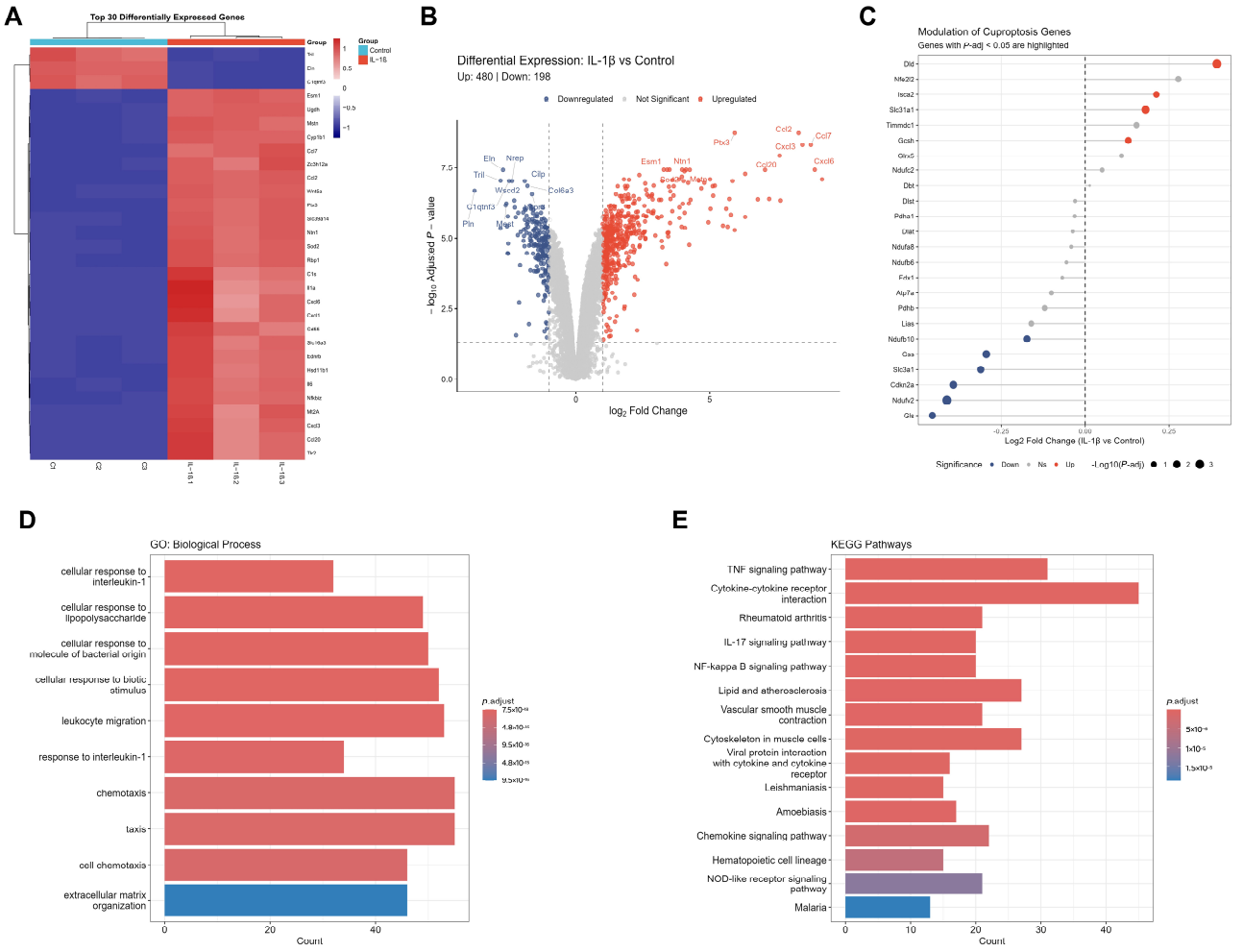

Figure 1. IL-1β primarily triggers an inflammatory transcriptomic response in rat TPCs, with modest alterations in selected cuproptosis-related genes. (**A**) Heatmap displaying the top 30 DEGs between control and IL-1β-treated samples. (**B**) Volcano plot illustrating genome-wide differential gene expression, with red and blue indicating genes that meet the specified upregulation and downregulation criteria, respectively. (**C**) Changes in expression of the predefined cuproptosis-associated genes. None of these genes fulfilled the combined adjusted criteria for genome-wide DEGs; the highlighted ones showed adjusted $p < 0.05$ with modest fold changes. (**D**) GO biological process enrichment analysis of the entire DEG set. (**E**) KEGG pathway enrichment analysis of the entire DEG set.

3.2. Gene Set Enrichment Analysis Reveals Coordinated Inflammatory Activation and Suppression of Structural Programs in IL-1β-Treated TPCs

To analyze coordinated transcriptomic changes beyond individual genes meeting the preset differential-expression thresholds, we conducted GSEA on the entire ranked gene list from IL-1β-treated and control rat TPCs. Positive NES indicates enrichment in IL-1β-treated cells, while negative NES values indicate enrichment in control cells and suppression after IL-1β treatment. GO: BP GSEA showed a strong positive enrichment for processes linked to the response to lipopolysaccharide, cellular response to lipopolysaccharide, response to bacterial molecules, cellular response to biotic stimuli, response to bacteria, and cellular

response to interleukin-1 (Figure 2A). Enrichment profiles confirmed that genes involved in these processes were mainly located toward the IL-1β-related end of the ranked gene list (Figure 2B). The presence of bacterial stimulus-related annotations indicates a significant overlap between IL-1β signaling pathways and conserved innate immune-response programs. In contrast, GO: BP terms linked to the regulation of potassium-ion transmembrane transport, pericyte differentiation, actomyosin structure organization, sarcomere organization, and muscle tissue morphogenesis were negatively enriched (Figure 2A). This indicates that inflammatory activation was associated with decreased expression of gene programs responsible for cytoskeletal organization, ion transport, and the maintenance of cellular structural homeostasis. KEGG GSEA showed a consistent pattern. Pathways like cytokine–cytokine receptor interaction, IL-17 signaling, TNF signaling, chemokine signaling, rheumatoid arthritis, lipid and atherosclerosis, and legionellosis were enriched in IL-1β-treated TPCs (Figure 2C). Enrichment profiles of key pathways confirmed coordinated activation of gene programs related to cytokines, chemokines, IL-17, and TNF (Figure 2D). Disease-associated pathways such as rheumatoid arthritis, lipid and atherosclerosis, and legionellosis should be viewed as groups of shared inflammatory genes, not evidence of these diseases occurring in TPCs. Overall, the GSEA results show that IL-1β promotes coordinated activation of inflammatory and innate immune response pathways while simultaneously downregulating programs related to structure, the cytoskeleton, and ion transport in rat TPCs. These findings provide a comprehensive view of the transcriptional environment associated with IL-1β-induced TPC dysfunction.

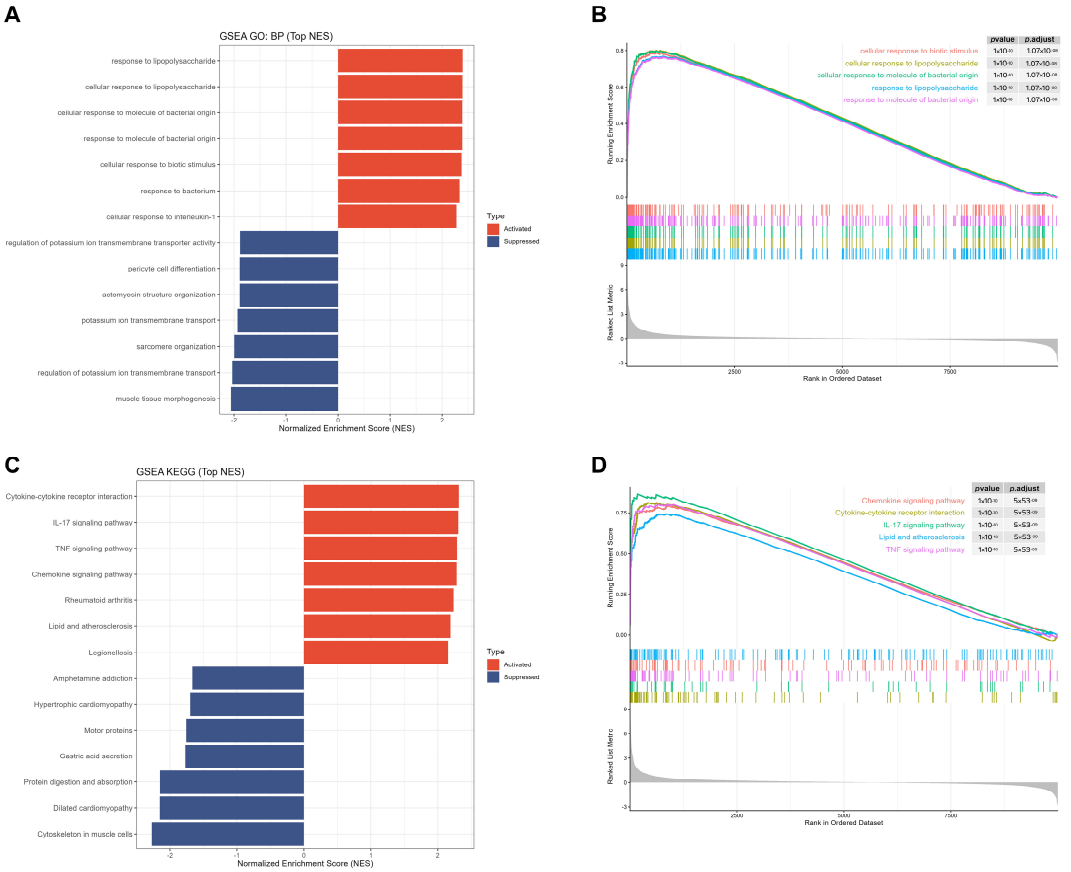

Figure 2. Gene set enrichment analysis (GSEA) of IL-1β-induced transcriptomic changes in rat tendon progenitor cells (TPCs). GSEA was conducted on the complete ranked gene list comparing IL-1β-treated and control rat TPCs. (**A**) Top GO: BP pathways with the highest positive and negative normalized enrichment scores (NES). (**B**) Running-enrichment profiles of key positively enriched GO: BP terms relating to cellular responses to interleukin-1, lipopolysaccharide, bacterial molecules, and

biotic stimuli. (**C**) KEGG pathways with the highest positive and negative NES values. (**D**) Running-enrichment profiles of notable positively enriched KEGG pathways, including chemokine signaling, cytokine–cytokine receptor interaction, IL-17 signaling, lipid and atherosclerosis, and TNF signaling. In panels (**A**,**C**), red shows gene sets positively enriched in IL-1β-treated cells, while blue indicates gene sets enriched in controls and suppressed after IL-1β treatment. In panels (**B**,**D**), the running enrichment score is plotted along the ranked gene list, with vertical ticks indicating the positions of individual genes within each set. *p* values are corrected for multiple testing using the Benjamini–Hochberg method.

3.3. IL-1β Induces an Inflammatory, Catabolic Phenotype and Alters Selected Mitochondrial Metabolic Genes in Rat TPCs

We characterized primary rat TPCs at passage 2–3, as previously reported [32]. The cells exhibited a typical mesenchymal stem cell antigen profile, characterized by CD73+, CD105+, and CD90+ expression, and by CD34− and CD45−. TPC populations < demonstrated robust multipotency, differentiating into adipogenic, osteogenic, and chondrogenic lineages under the appropriate induction conditions.

To establish an inflammatory model of TPC dysfunction, cells were stimulated with IL-1β, a key cytokine that drives ECM degradation [16,41,42]. The results showed that IL-1β significantly reduced CCK-8 metabolic activity compared with untreated controls ($p < 0.001$; Figure 3A). Treatment with IL-1β significantly reduced *Scx* expression ($p < 0.001$; Figure 3B). Furthermore, IL-1β significantly downregulated the structural matrix genes *Col1a1* and *Col3a1* ($p < 0.001$, Figure 3C,D) while upregulating pro-inflammatory and catabolic markers, including *Il-6*, *Mmp3*, and *Mmp13* ($p < 0.01$ and $p < 0.001$; Figure 3E–G), and elevated H_2DCF-DA fluorescence ($p < 0.001$, Figure 3H,I). These findings show that IL-1β induces a combined inflammatory, oxidative, catabolic, and tenogenic dysfunction phenotype in TPCs.

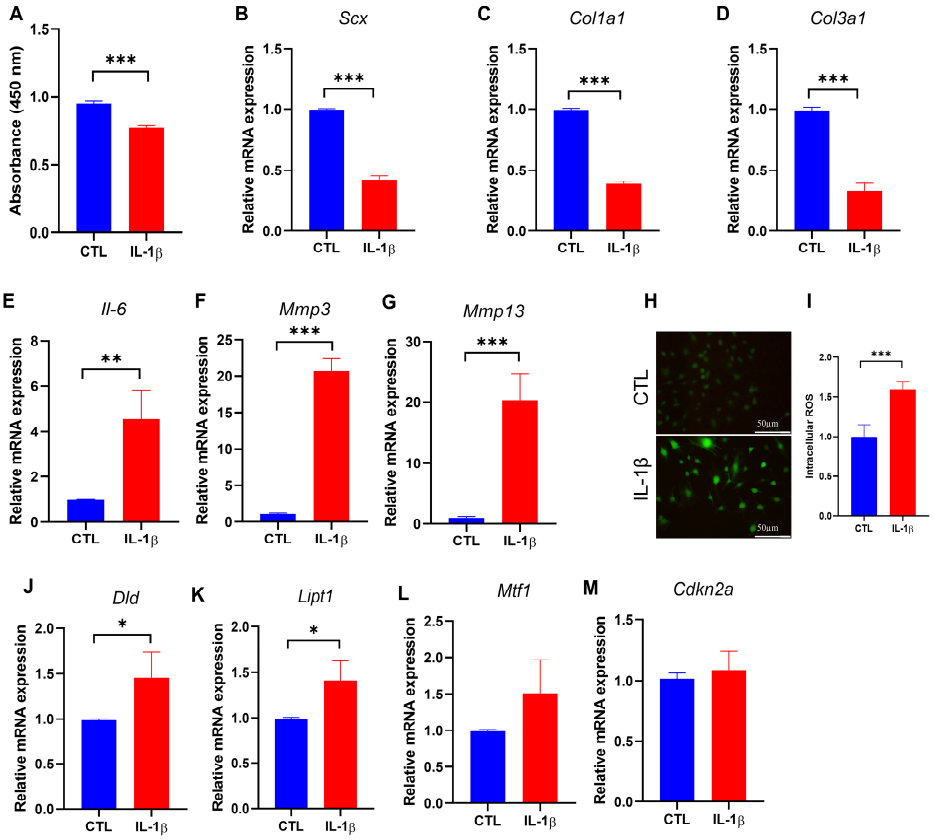

Figure 3. IL-1β induces inflammatory, catabolic, oxidative, tenogenic dysfunction, and alters selected cuproptosis-associated genes in rat TPCs. (**A**) CCK-8 metabolic activity in TPCs after IL-1β treatment

for 24 h. (**B**–**D**) Relative mRNA expression of the tenogenic and matrix-associated genes *Scx* (**B**), *Col1a1* (**C**), and *Col3a1* (**D**). (**E**–**G**) Relative mRNA expression of the inflammatory and catabolic genes *Il6* (**E**), *Mmp3* (**F**), and *Mmp13* (**G**). (**H**,**I**) Representative H_2DCF-DA fluorescence images and quantitative analysis after 24 h of IL-1β treatment. Scale bar, 50 µm. (**J**–**M**) Relative mRNA levels of *Dld* (**J**), *Lipt1* (**K**), *Mtf1* (**L**), and *Cdkn2a* (**M**) following IL-1β stimulation. Data are expressed as mean ± SD ($n = 3$). * $p < 0.05$, ** $p < 0.01$, *** $p < 0.001$.

We next examined whether IL-1β-induced TPC dysfunction was accompanied by altered expression of genes associated with mitochondrial lipoylation, copper-responsive stress, or cuproptosis. IL-1β significantly upregulated dihydrolipoamide dehydrogenase (*Dld*) and lipoyltransferase 1 (*Lipt1*) ($p < 0.05$; Figure 3J,K). *Dld* encodes a mitochondrial oxidoreductase that functions in several dehydrogenase complexes, whereas *Lipt1* encodes a mitochondrial lipoyltransferase required for protein lipoylation [43,44]. Meanwhile, metal regulatory transcription factor 1 (*Mtf1*) and cyclin-dependent kinase inhibitor 2A (*Cdkn2a*) remained unchanged (Figure 3L,M). The selective changes in *Dld* and *Lipt1*, together with the absence of significant changes in *Mtf1* and *Cdkn2a*, indicate limited rather than global transcriptional remodeling of the selected cuproptosis-associated gene set. The results suggest that inflammatory stress influences metabolic elements associated with cellular susceptibility to copper-related damage.

3.4. TTM Attenuates Selected Features of IL-1β-Induced TPC Dysfunction

To determine whether modulation of copper availability affected the IL-1β-induced phenotype, we treated TPCs with IL-1β and the high-affinity copper chelator TTM. Copper chelation has been reported to reduce the cellular damage caused by inflammation [45]. TTM cotreatment increased CCK-8 metabolic activity relative to cells treated with IL-1β alone ($p < 0.01$, Figure 4A). TTM also attenuated the IL-1β-associated reduction in *Scx* and *Col1a1* expression ($p < 0.01$), whereas *Col3a1* was not (Figure 4B–D). The IL-1β-associated increases in Dld and *Lipt1* expression were reduced by TTM cotreatment ($p < 0.05$ and $p < 0.001$; Figure 4E,F). Additionally, the elevated intracellular ROS levels were significantly reduced by TTM co-treatment ($p < 0.001$; Figure 4G,H). These findings suggest that chelating copper affects certain metabolic, oxidative, and tenogenic responses to IL-1β. However, because TTM may also affect copper-dependent enzymes, redox processes, and inflammatory signaling more broadly, its protective effect alone does not definitively demonstrate inhibition of cuproptosis.

3.5. Pharmacological Copper Loading with ES + Cu Stress Causes a TTM-Sensitive TPC Dysfunction Phenotype

To determine whether TPCs were susceptible to experimentally induced copper-dependent stress, cells were exposed to $CuCl_2$ and the copper ionophore elesclomol (ES). In this study, $CuCl_2$ (Cu) treatment reduced CCK-8 metabolic activity in a concentration-dependent manner (Figure 5A), while ES alone did not significantly alter metabolic activity at the tested concentrations (Figure 5B). The combination of ES + Cu significantly reduced CCK-8 metabolic activity, and this effect was attenuated by cotreatment with TTM (Figure 5C).

Treatment of TPCs with a combination of ES and Cu significantly reduced the expression of the tenogenic genes *Scx* and *Col1a1* ($p < 0.05$, $p < 0.01$, Figure 5D,E), which was increased by cotreatment with TTM ($p < 0.01$, $p < 0.05$, Figure 5D,E). ES and Cu increased *Dld* and *Lipt1* expression ($p < 0.05$, Figure 5F,G), which was reduced by cotreatment with TTM ($p < 0.05$, $p < 0.01$, Figure 5F,G). In addition, ES + Cu increased H_2DCF-DA fluorescence, which was reduced by cotreatment with TTM ($p < 0.001$; Figure 5H,I). Therefore, pharmacologically increasing intracellular copper levels led to a copper-chelator-sensitive phenotype characterized by reduced metabolic activity, suppression of tenogenic gene expression, alterations in mitochondrial metabolic genes, and increased oxidative stress. This phenotype shares some features with IL-1β-induced TPC dysfunction. However, decreased CCK-8 activity, ROS

accumulation, and TTM sensitivity are not exclusive to cuproptosis. Therefore, the ES + Cu condition is regarded as a pharmacological stress model consistent with cuproptosis, rather than as conclusive evidence of cuproptotic cell death.

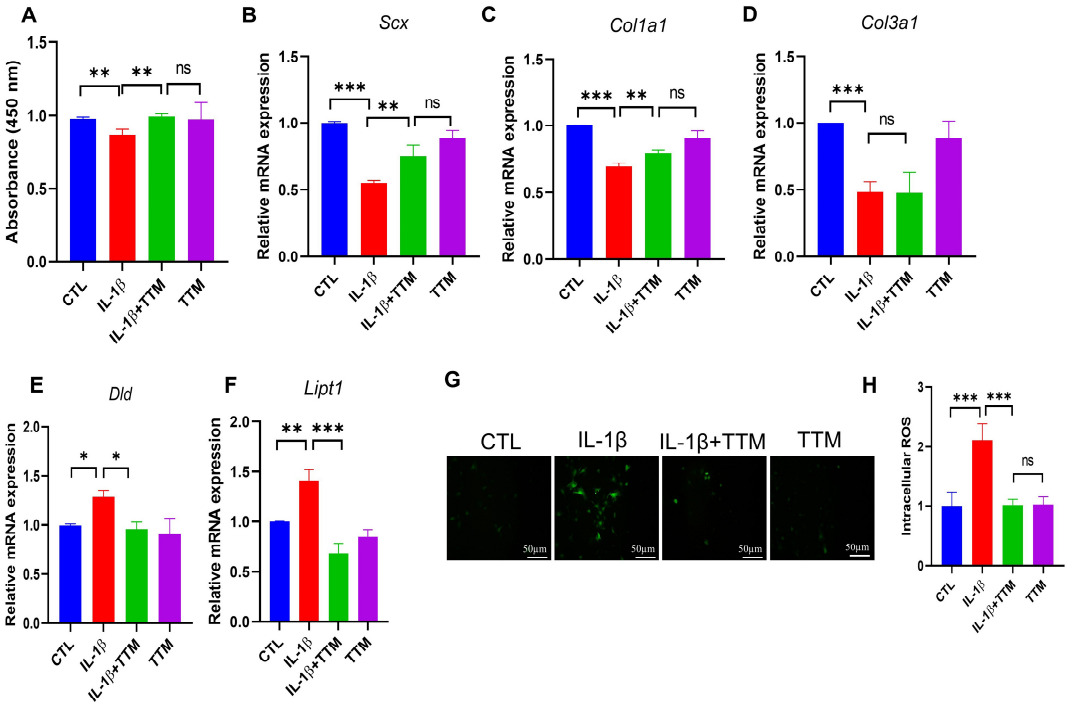

Figure 4. TTM attenuates IL-1β-associated changes in metabolic activity, mitochondrial metabolic genes, and ROS-associated fluorescence. (**A**) CCK-8 assay measuring metabolic activity in the control, IL-1β-treated, IL-1β/TTM co-treated, and TTM-only groups. (**B**–**D**) Relative mRNA levels of *Scx* (**B**), *Col1a1* (**C**), and *Col3a1* (**D**). (**E**,**F**) Relative mRNA expression of *Dld* (**E**) and *Lipt1* (**F**) in control, IL-1β-treated, and IL-1β/TTM-cotreated TPCs. (**G**,**H**) Representative H_2DCF-DA fluorescence images and quantitative analysis under the corresponding conditions. Scale bar, 50 μm. Data are shown as mean ± SD (n = 3). * $p < 0.05$, ** $p < 0.01$, *** $p < 0.001$. ns: not significant.

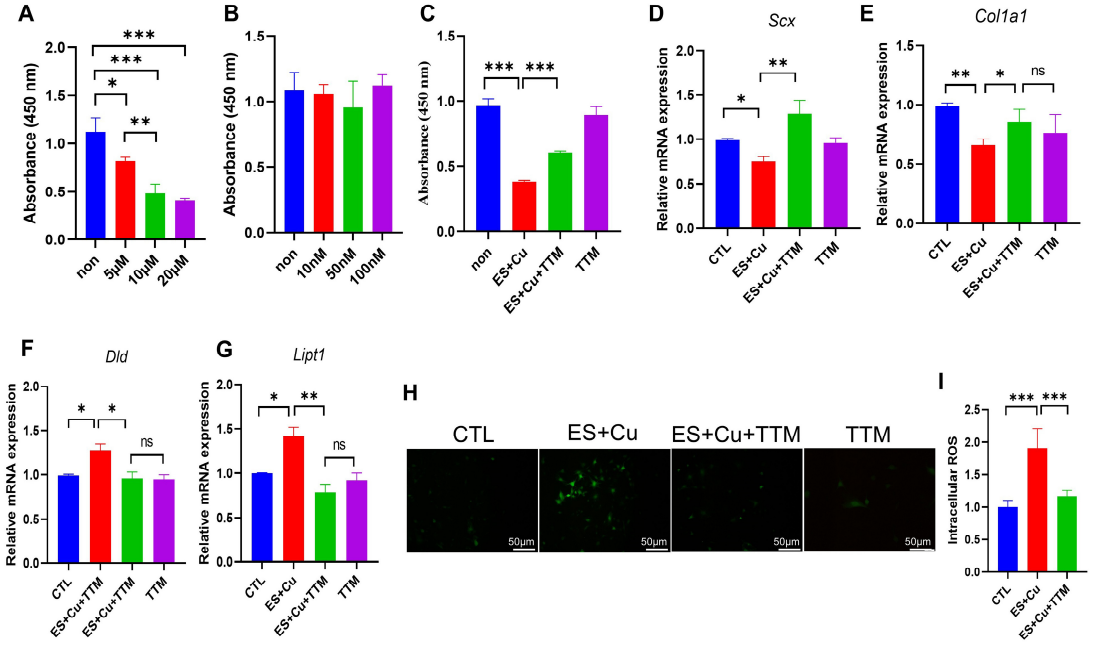

Figure 5. Pharmacological induction of ES + Cu stress causes a TTM-sensitive dysfunction phenotype in TPCs. (**A**) Effect of $CuCl_2$ concentration on TPC CCK-8 metabolic activity after 24 h. (**B**) Impact of

ES alone on CCK-8 metabolic activity. (**C**) CCK-8 metabolic activity following combined ES + Cu exposure, in the presence or absence of TTM. (**D**–**G**) Relative mRNA levels of *Scx* (**D**), *Col1a1* (**E**), *Dld* (**F**), and *Lipt1* (**G**) after ES/Cu treatment, with or without TTM. (**H**,**I**) Typical H_2DCF-DA fluorescence images and quantitative data illustrating the effects of ES + Cu and TTM, with a 50 μm scale bar. Green signals denote H_2DCF-DA fluorescence. Data are shown as mean ± SD (n = 3). * $p < 0.05$, ** $p < 0.01$, *** $p < 0.001$. ns: not significant.

3.6. Human TPC Single-Cell Analysis Reveals Condition-Related Changes in Mitochondrial Lipoylation Gene Expression

To investigate whether related transcriptional patterns were present in human tendon-derived cells, we analyzed single-cell RNA-sequencing data from GSE150482. The dataset comprised cultured human patellar tendon-derived progenitor cells from three biological donors per condition, including the experimental mechanical-stimulation conditions described in the original study [29]. After quality control, sample assignment, and scVI-based integration, we used UMAP visualization to examine the cellular distribution across conditions (Figure 6A).

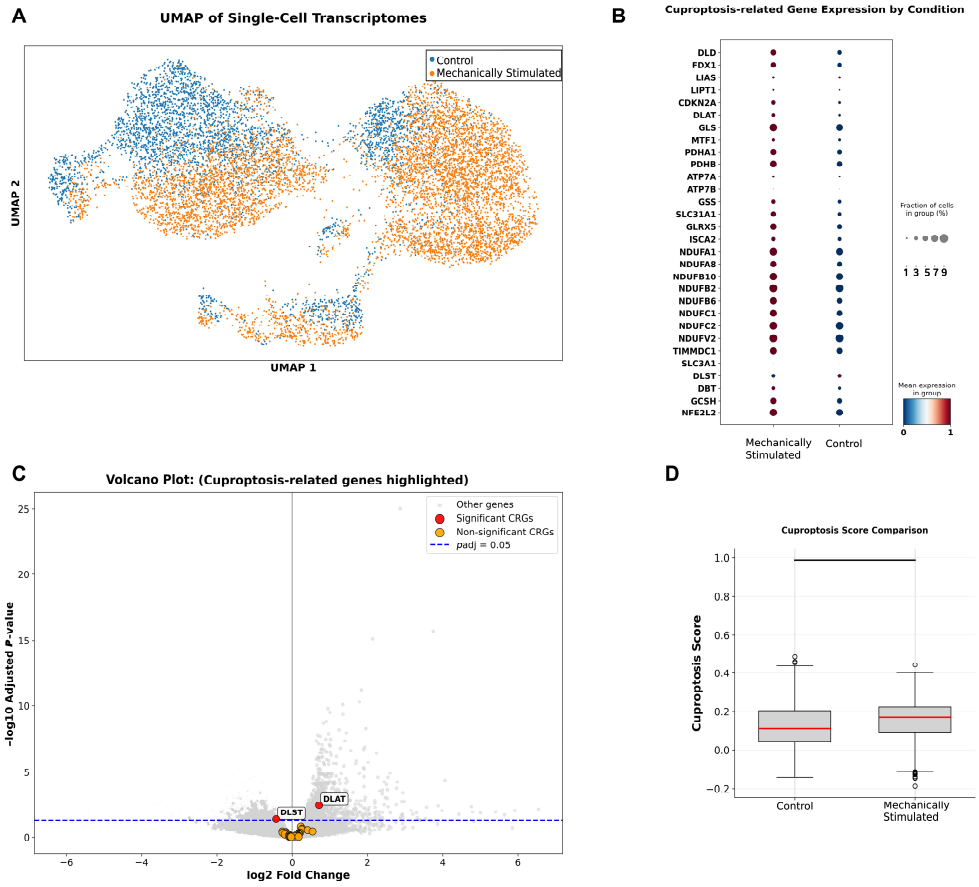

Figure 6. Mechanical stimulation links to changes in mitochondrial and cuproptosis-related genes in cultured human TPCs. (**A**) UMAP plot of integrated single-cell data from control and mechanically stimulated cultures, with each point indicating a single cell; three biological donors per condition were analyzed. (**B**) Dot plot showing expression levels of genes associated with copper regulation, mitochondrial function, protein lipoylation, and cuproptosis. Dot size shows the percentage of cells expressing each gene, while color indicates average expression. (**C**) Differential expression analysis at the donor level between experimental conditions, focusing on cuproptosis-associated genes such as DLAT and DLST. (**D**) Expression scores for cuproptosis-related pathways across conditions, reflecting pathway activity rather than a direct measure of cell death.

A dot plot of the predefined cuproptosis-associated gene set showed condition-dependent differences in genes involved in mitochondrial metabolism, protein lipoylation, and copper-responsive pathways (Figure 6B). To quantitatively evaluate these changes while accounting for biological replication, we conducted differential expression analysis using a pseudobulk approach (n = 3 control cultures vs. n = 3 mechanically stimulated cultures) rather than treating individual cells as independent observations. Among the evaluated genes, DLAT (Dihydrolipoamide S-acetyltransferase), the E2 subunit of the pyruvate dehydrogenase complex and a key protein involved in copper-induced aggregation, was increased, whereas DLST, which encodes the E2 component of the α-ketoglutarate dehydrogenase complex, was decreased under the compared condition (Figure 6C). The opposing regulation of these mitochondrial enzyme transcripts suggests remodeling of mitochondrial TCA-cycle-associated metabolism. However, measuring transcript levels does not prove DLAT lipoylation, copper binding, protein aggregation, or cuproptotic activity. A composite cuproptosis-related expression score was also assessed (Figure 6D). Since this score combines genes involved in copper transport, mitochondrial metabolism, lipoylation, and stress responses, it is better considered as an indicator of pathway-related transcription rather than a direct measure of cuproptosis. The observed differences suggest remodeling of a copper- and/or cuproptosis-associated transcriptional program in human tendon-derived cells, but they do not confirm the occurrence of cuproptotic cell death.

4. Discussion

Tendinopathy develops through interactions among mechanical loading, ECM disruption, inflammation, oxidative stress, and impaired cellular repair. In this study, IL-1β induced an inflammatory TPC dysfunction phenotype characterized by reduced metabolic activity, suppression of tenogenic and matrix-associated genes, induction of catabolic and inflammatory transcripts, and increased ROS-associated fluorescence. The principal additional finding was that this phenotype was accompanied by altered expression of selected genes involved in mitochondrial lipoylation and cuproptosis-associated metabolism, and that it was partially modified by copper chelation. Pharmacologically induced ES + Cu stress produced an overlapping TTM-sensitive phenotype. These results link inflammatory TPC dysfunction with copper-sensitive mitochondrial stress, but do not establish endogenous cuproptotic cell death.

The rat transcriptomic analysis further contextualized the experimental findings within a broader inflammatory framework. IL-1β induced significant transcriptional changes, primarily in chemokines, cytokine signaling, and the TNF, IL-17, and NF-κB pathways [36,37,39,40]. In contrast, the changes in the selected cuproptosis-related genes were minor, with none meeting the criteria for genome-wide differential expression based on fold change and adjusted p-value. GO enrichment for response to hypoxia is particularly important for tendon biology. Since tendons are naturally hypovascular and hypoxic, the combination of hypoxia-induced stress and inflammatory signals likely lowers the threshold at which the cellular copper becomes toxic to TPCs [35,46]. GO: BP GSEA also showed positive enrichment in responses to lipopolysaccharide, bacterial molecules, and biotic stimuli. These annotations highlight the significant overlap between IL-1β signaling and conserved innate immune transcriptional programs. Alongside the enrichment of cytokine- and chemokine-related KEGG pathways, these findings suggest that IL-1β restructures multiple interconnected inflammatory networks instead of triggering a single isolated pathway. Simultaneously, the negative enrichment of gene sets related to the cytoskeleton, motor proteins, actomyosin organization, ion transport, and tissue development indicates that inflammatory activation is linked with decreased expression of genes responsible for cellular structure and stability. This downregulation of structural programs aligns with

the observed decrease in *Scx* and collagen expression and suggests a shift away from a tenogenic, homeostatic state.

The transcriptomic results primarily provide contextual, rather than mechanistic, insights into copper-dependent cell death. The top GSEA outcomes highlighted inflammatory and structural processes instead of specific pathways related to copper homeostasis, mitochondrial protein lipoylation, or cuproptosis. These results indicate that inflammation is the main transcriptional response, while the copper- and/or cuproptosis-related signal is relatively indirect. Although broad inflammatory pathways are enriched, this does not confirm cuproptosis; rather, it may indicate a metabolic environment that influences how cells respond to copper. This remains a hypothesis that needs direct mechanistic testing.

The IL-1β model replicates key cellular features of tendinopathy. Downregulation of *Scx*, *Col1a1*, and *Col3a1* reflects reduced tenogenic and matrix-related gene expression, while elevated levels of *Il6*, *Mmp3*, and *Mmp13* indicate a shift toward an inflammatory and catabolic state. These findings are consistent with previous evidence that inflammatory cytokines compromise the tenogenic functions of tendon-derived progenitor cells [16,42]. The increased H_2DCF-DA fluorescence suggests that the inflammatory response was linked to higher intracellular oxidative activity [20]. However, IL-1β stimulation is only one component of the complex tendinopathy environment and does not recapitulate the mechanical loading, matrix disorganization, vascular alterations, and immune-cell interactions observed in vivo [14]. IL-1β also increased the expression of *Dld* and *Lipt1*, whereas *Mtf1* and *Cdkn2a* remained unchanged. *Dld* participates in multiple mitochondrial dehydrogenase complexes, and *Lipt1* is required for the lipoylation of mitochondrial proteins [43,44,47]. These processes are relevant to cuproptosis because copper-dependent cell death occurs through interactions between copper and lipoylated TCA-cycle proteins [28]. However, *Dld* and *Lipt1* are involved in normal mitochondrial functions and are not specific indicators of cuproptosis. Changes in their expression are better understood as evidence that IL-1β affects mitochondrial metabolism, potentially increasing susceptibility to copper-related stress. The absence of changes in *Mtf1* and *Cdkn2a* also suggests that the response does not involve direct activation of a specific cuproptosis gene program.

TTM cotreatment mitigated the IL-1β-induced decrease in CCK-8 metabolic activity, restored the expression of *Scx* and *Col1a1*, decreased *Dld* and *Lipt1* levels, and reduced ROS-related fluorescence. These results show that altering copper availability can impact specific responses to inflammatory stress. However, TTM is not a pathway-specific inhibitor of cuproptosis; copper chelation can influence copper-dependent enzymes, oxidative balance, mitochondrial function, and inflammatory pathways independently of cuproptosis [48]. The varied response of tenogenic genes indicates that TTM did not fully restore TPC identity. While TTM attenuated the decrease in *Scx* and *Col1a1*, it did not significantly improve *Col3a1* levels. Rather than showing that cuproptosis selectively controls mature collagen, this suggests that different matrix-related genes react differently to copper chelation. The regulation of *Col3a1* may still be mainly influenced by inflammatory, stress, or matrix-remodeling pathways that remain largely unaffected by the current treatment. Therefore, the data suggest only a partial modification, not complete reversal, of the IL-1β-induced phenotype.

The ES + Cu experiment provided additional pharmacological evidence that TPCs are affected by elevated copper levels. While ES alone did not significantly affect CCK-8 metabolic activity, the ES + Cu combination caused a notable decrease, which TTM mitigated. This combination also downregulated tenogenic genes, increased *Dld* and *Lipt1* expression, and increased ROS-related fluorescence. The similarity to the IL-1β response suggests possible common pathways involving mitochondrial or oxidative stress. However, because CCK-8 reduction and H_2DCF-DA fluorescence are not pathway-specific, injury

from ES + Cu may result from multiple copper-dependent toxic effects. Without direct assessments of lipoylated protein aggregation, iron–sulfur cluster protein loss, proteotoxic stress, or genetic dependence on lipoylation machinery, the ES + Cu phenotype is consistent with, but does not definitively prove, cuproptosis.

Analysis of the human single-cell dataset revealed condition-related alterations in mitochondrial metabolic and protein-lipoylation-associated genes, with increased DLAT and decreased DLST. These genes encode lipoylated E2 subunits of mitochondrial dehydrogenases, making them biologically significant for copper-sensitive mitochondrial function [28,49]. However, increased DLAT transcript levels do not indicate increased protein lipoylation or aggregation. Likewise, the cuproptosis-related expression score combines transcriptional data from a diverse set of genes and should not be taken as a direct indicator of cell death. Therefore, human data provide cross-species evidence of changes in mitochondrial metabolic pathways in stressed tendon-derived progenitor cells, but they do not provide clinical or mechanistic confirmation of cuproptosis in human tendinopathy.

Overall, the experimental and transcriptomic findings support a model in which IL-1β triggers a mainly inflammatory and oxidative TPC dysfunction phenotype, with secondary effects on mitochondrial and copper-responsive gene remodeling. Pharmacological copper loading elicits a similar stress response, whereas copper chelation attenuates some of these responses in both cases. These observations suggest that copper-sensitive mitochondrial stress may contribute to TPC dysfunction. However, they do not prove that endogenous copper accumulation causes tendinopathy or that cuproptosis is the main form of cell death.

Several limitations should be noted. First, measurements of intracellular copper levels and distribution were not performed. Second, key biochemical signs of cuproptosis, such as lipoylated DLAT aggregation, destabilization of iron–sulfur cluster proteins, and proteotoxic stress, were not investigated. Third, TTM may have biological effects beyond inhibiting cuproptosis, and not all pharmacological treatments included complete factorial controls. Fourth, the transcriptomic analyses identify associations rather than causal relationships, and the gene set linked to cuproptosis also includes genes involved in broader mitochondrial and stress-response processes. Despite these limitations, the study has several strengths. It integrated transcriptomic analysis with targeted in vitro experiments on primary, well-characterized rat TPCs, enabling functional assessment of transcriptomic findings. In addition, rat bulk RNA-seq data were analyzed using both threshold-based differential expression and threshold-free GSEA, offering complementary insights at the gene and pathway levels regarding the IL-1β response. Moreover, copper sensitivity was evaluated in two ways: by copper loading with ES + Cu and by copper chelation with TTM. TTM responsiveness was observed in both the IL-1β and ES + Cu models. Subsequent studies should determine whether endogenous copper handling is altered under inflammatory or mechanical stress and whether established cuproptosis-associated biochemical changes occur in TPCs. Until such evidence is available, the present findings are best interpreted as demonstrating a cuproptosis-associated, copper-sensitive stress phenotype.

5. Conclusions

IL-1β triggered inflammatory, catabolic, oxidative, and tenogenic dysfunction in rat TPCs and affected the expression of specific genes involved in mitochondrial lipoylation and cuproptosis-related metabolism. Copper chelation with TTM reduced several aspects of this phenotype, whereas pharmacologically induced ES + Cu stress elicited similar metabolic, transcriptional, and oxidative changes that also responded to TTM. Both rat bulk and human single-cell transcriptomic analyses revealed further alterations in inflammatory and mitochondrial metabolic pathways. These findings suggest an association between inflammatory TPC dysfunction and copper-sensitive mitochondrial stress. Therefore,

mechanisms related to cuproptosis should be regarded as a potential factor in TPC dysfunction to be tested, rather than as a confirmed cause of tendinopathy.

Supplementary Materials: The following supporting information can be downloaded at https://www.mdpi.com/article/10.3390/antiox15111371/s1, Table S1: A curated list of genes associated with cuproptosis, copper homeostasis, mitochondrial lipoylation, and copper-dependent stress responses.

Author Contributions: M.Z.: Writing—original draft, Methodology, Investigation, Conceptualization, Writing—review and editing. H.K.: Investigation, Methodology. H.T.: Investigation, Formal analysis, and Writing—review and editing. B.-H.J.: Writing—review and editing, Supervision. All authors have read and agreed to the published version of the manuscript.

Funding: This work was supported by National Research Foundation of Korea (NRF) grants funded by the Korean government (MSIT) (RS-2025-23963916, RS-2025-00517133, and RS-2025-24792972) and a Korea Basic Science Institute (National Research Facilities and Equipment Center) grant funded by the Ministry of Education (grant No. RS-2021-NF000550).

Institutional Review Board Statement: The study was approved by the Animal Care and Use Committee (IACUC) of Jeonbuk National University (NON2024-093; approval date: 29 July 2024). All experiments were performed in accordance with the guidelines and regulations of the Animal Care Committee at Jeonbuk National University.

Informed Consent Statement: Not applicable.

Data Availability Statement: Publicly available datasets were downloaded and analyzed in this study and are available in GEO under accession numbers GSE253913 and GSE150482. Experimental data generated in this study are available from the corresponding author upon reasonable request.

Acknowledgments: While preparing this manuscript, the authors used ChatGPT 5.6 only for English-language editing, such as improving grammar, clarity, and readability. The tool was not used for data generation, analysis, interpretation of results, or the formation of scientific conclusions. All AI-assisted content has been thoroughly reviewed and edited by the authors, who assume full responsibility for the publication.

Conflicts of Interest: The authors declare no conflicts of interest.

References

1. Jeon, H.; McGrath, M.L.; Grandgenett, N.; Rosen, A.B. Clinical Measures and Their Contribution to Dysfunction in Individuals With Patellar Tendinopathy. *J. Sport Rehabil.* **2019**, *28*, 165–170. [CrossRef] [PubMed]
2. Hopkins, C.; Fu, S.-C.; Chua, E.; Hu, X.; Rolf, C.; Mattila, V.M.; Qin, L.; Yung, P.S.-H.; Chan, K.-M. Critical review on the socio-economic impact of tendinopathy. *Asia-Pac. J. Sports Med. Arthrosc. Rehabil. Technol.* **2016**, *4*, 9–20. [CrossRef] [PubMed]
3. Andres, B.M.; Murrell, G.A. Treatment of tendinopathy: What works, what does not, and what is on the horizon. *Clin. Orthop. Relat. Res.* **2008**, *466*, 1539–1554. [CrossRef] [PubMed]
4. Larsson, M.E.; Käll, I.; Nilsson-Helander, K. Treatment of patellar tendinopathy--a systematic review of randomized controlled trials. *Knee Surg. Sports Traumatol. Arthrosc.* **2012**, *20*, 1632–1646. [CrossRef]
5. Rudavsky, A.; Cook, J. Physiotherapy management of patellar tendinopathy (jumper's knee). *J. Physiother.* **2014**, *60*, 122–129. [CrossRef] [PubMed]
6. Nuhmani, S. Injection therapies for patellar tendinopathy. *Phys. Sportsmed.* **2020**, *48*, 125–130. [CrossRef] [PubMed]
7. Challoumas, D.; Clifford, C.; Kirwan, P.; Millar, N.L. How does surgery compare to sham surgery or physiotherapy as a treatment for tendinopathy? A systematic review of randomised trials. *BMJ Open Sport. Exerc. Med.* **2019**, *5*, e000528. [CrossRef]
8. Trapana, J.; Weinerman, J.; Lee, D.; Sedani, A.; Constantinescu, D.; Best, T.M.; Hornicek, F.J., Jr.; Hare, J.M. Cell-based therapy in the treatment of musculoskeletal diseases. *Stem Cells Transl. Med.* **2024**, *13*, 959–978. [CrossRef] [PubMed]
9. Mahmoud, E.E.; Mawas, A.S.; Mohamed, A.A.; Noby, M.A.; Abdel-Hady, A.A.; Zayed, M. Treatment strategies for meniscal lesions: From past to prospective therapeutics. *Regen. Med.* **2022**, *17*, 547–560. [CrossRef] [PubMed]
10. Zayed, M.; Adair, S.; Dhar, M. Effects of Normal Synovial Fluid and Interferon Gamma on Chondrogenic Capability and Immunomodulatory Potential Respectively on Equine Mesenchymal Stem Cells. *Int. J. Mol. Sci.* **2021**, *22*, 6391. [CrossRef] [PubMed]

11. Fraile, M.; Eiro, N.; Costa, L.A.; Martín, A.; Vizoso, F.J. Aging and Mesenchymal Stem Cells: Basic Concepts, Challenges and Strategies. *Biology* **2022**, *11*, 1678. [CrossRef] [PubMed]
12. Zayed, M.; Iohara, K. Effects of p-Cresol on Senescence, Survival, Inflammation, and Odontoblast Differentiation in Canine Dental Pulp Stem Cells. *Int. J. Mol. Sci.* **2020**, *21*, 6931. [CrossRef] [PubMed]
13. Abate, M.; Silbernagel, K.G.; Siljeholm, C.; Di Iorio, A.; De Amicis, D.; Salini, V.; Werner, S.; Paganelli, R. Pathogenesis of tendinopathies: Inflammation or degeneration? *Arthritis Res. Ther.* **2009**, *11*, 235. [CrossRef] [PubMed]
14. Millar, N.L.; Silbernagel, K.G.; Thorborg, K.; Kirwan, P.D.; Galatz, L.M.; Abrams, G.D.; Murrell, G.A.C.; McInnes, I.B.; Rodeo, S.A. Tendinopathy. *Nat. Rev. Dis. Primers* **2021**, *7*, 1. [CrossRef] [PubMed]
15. Jomaa, G.; Kwan, C.K.; Fu, S.C.; Ling, S.K.; Chan, K.M.; Yung, P.S.; Rolf, C. A systematic review of inflammatory cells and markers in human tendinopathy. *BMC Musculoskelet. Disord.* **2020**, *21*, 78. [CrossRef] [PubMed]
16. Mobasheri, A.; Shakibaei, M. Is tendinitis an inflammatory disease initiated and driven by pro-inflammatory cytokines such as interleukin 1β? *Histol. Histopathol.* **2013**, *28*, 955–964. [CrossRef] [PubMed]
17. Xia, X.; Fang, Z.; Qian, Y.; Zhou, Y.; Huang, H.; Xu, F.; Luo, Z.; Wang, Q. Role of oxidative stress in the concurrent development of osteoporosis and tendinopathy: Emerging challenges and prospects for treatment modalities. *J. Cell. Mol. Med.* **2024**, *28*, e18508. [CrossRef] [PubMed]
18. Pizzino, G.; Irrera, N.; Cucinotta, M.; Pallio, G.; Mannino, F.; Arcoraci, V.; Squadrito, F.; Altavilla, D.; Bitto, A. Oxidative Stress: Harms and Benefits for Human Health. *Oxid. Med. Cell. Longev.* **2017**, *2017*, 8416763. [CrossRef] [PubMed]
19. Yuan, T.; Qian, H.; Yu, X.; Meng, J.; Lai, C.T.; Jiang, H.; Zhao, J.N.; Bao, N.R. Proteomic analysis reveals rotator cuff injury caused by oxidative stress. *Ther. Adv. Chronic Dis.* **2021**, *12*, 2040622320987057. [CrossRef] [PubMed]
20. Kračun, D.; Görlach, A.; Snedeker, J.G.; Buschmann, J. Reactive oxygen species in tendon injury and repair. *Redox Biol.* **2025**, *81*, 103568. [CrossRef] [PubMed]
21. Abate, M.; Di Carlo, L.; Cocco, G.; Cocco, A.; Sabatini, E.; Salini, V. Oxidative Stress and Abnormal Tendon Sonographic Features in Elite Soccer Players (A Pilot Study). *Rev. Bras. Ortop.* **2021**, *56*, 432–437. [CrossRef] [PubMed]
22. Festa, R.A.; Thiele, D.J. Copper: An essential metal in biology. *Curr. Biol.* **2011**, *21*, R877–R883. [CrossRef] [PubMed]
23. Ruiz, L.M.; Libedinsky, A.; Elorza, A.A. Role of Copper on Mitochondrial Function and Metabolism. *Front. Mol. Biosci.* **2021**, *8*, 711227. [CrossRef] [PubMed]
24. Kardos, J.; Héja, L.; Simon, Á.; Jablonkai, I.; Kovács, R.; Jemnitz, K. Copper signalling: Causes and consequences. *Cell Commun. Signal.* **2018**, *16*, 71. [CrossRef] [PubMed]
25. Han, J.; Luo, J.; Wang, C.; Kapilevich, L.; Zhang, X.-A. Roles and mechanisms of copper homeostasis and cuproptosis in osteoarticular diseases. *Biomed. Pharmacother.* **2024**, *174*, 116570. [CrossRef] [PubMed]
26. Manto, M. Abnormal Copper Homeostasis: Mechanisms and Roles in Neurodegeneration. *Toxics* **2014**, *2*, 327–345. [CrossRef]
27. Chen, L.; Min, J.; Wang, F. Copper homeostasis and cuproptosis in health and disease. *Signal Transduct. Target. Ther.* **2022**, *7*, 378. [CrossRef] [PubMed]
28. Tsvetkov, P.; Coy, S.; Petrova, B.; Dreishpoon, M.; Verma, A.; Abdusamad, M.; Rossen, J.; Joesch-Cohen, L.; Humeidi, R.; Spangler, R.D.; et al. Copper induces cell death by targeting lipoylated TCA cycle proteins. *Science* **2022**, *375*, 1254–1261. [CrossRef] [PubMed]
29. Still, C., 2nd; Chang, W.T.; Sherman, S.L.; Sochacki, K.R.; Dragoo, J.L.; Qi, L.S. Single-cell transcriptomic profiling reveals distinct mechanical responses between normal and diseased tendon progenitor cells. *Cell Rep. Med.* **2021**, *2*, 100343. [CrossRef] [PubMed]
30. Liu, H. Pan-cancer profiles of the cuproptosis gene set. *Am. J. Cancer Res.* **2022**, *12*, 4074–4081. [CrossRef] [PubMed]
31. Chang, B.; Hu, Z.; Chen, L.; Jin, Z.; Yang, Y. Development and validation of cuproptosis-related genes in synovitis during osteoarthritis progress. *Front. Immunol.* **2023**, *14*, 1090596. [CrossRef] [PubMed]
32. Khaled, H.; Zayed, M.; Kim, B.; Jeong, B.-H.; Oh, S.-I. Enhanced tenogenic potential of tendon-derived mesenchymal stem cells: Transcriptomic profiling and in vivo validation. *Front. Cell Dev. Biol.* **2025**, *13*, 1687816. [CrossRef] [PubMed]
33. Khaled, H.; Zayed, M.; Kim, B.; Jeong, B.H.; Oh, S.I. Decellularized tendon scaffold seeded with adipose-derived MSCs and supplemented with G-CSF injection promotes tendon repair in a rat model. *Biomed. Pharmacother.* **2026**, *202*, 119798. [CrossRef] [PubMed]
34. Khaled, H.; Zayed, M.; Kim, B.; Jeong, B.-H.; Oh, S.-I. Transcriptomic and functional comparison of adipose-and bone marrow-derived mesenchymal stem cells for tendon regeneration. *Stem Cell Res. Ther.* **2026**, *17*, 130. [CrossRef] [PubMed]
35. Tang, D.; Pu, B.; Liu, S.; Li, H. Identification of cuproptosis-associated subtypes and signature genes for diagnosis and risk prediction of Ulcerative colitis based on machine learning. *Front. Immunol.* **2023**, *14*, 1142215. [CrossRef] [PubMed]
36. Liao, Y.; Zhao, J.; Bulek, K.; Tang, F.; Chen, X.; Cai, G.; Jia, S.; Fox, P.L.; Huang, E.; Pizarro, T.T.; et al. Inflammation mobilizes copper metabolism to promote colon tumorigenesis via an IL-17-STEAP4-XIAP axis. *Nat. Commun.* **2020**, *11*, 900. [CrossRef] [PubMed]
37. Brady, D.C.; Crowe, M.S.; Turski, M.L.; Hobbs, G.A.; Yao, X.; Chaikuad, A.; Knapp, S.; Xiao, K.; Campbell, S.L.; Thiele, D.J.; et al. Copper is required for oncogenic BRAF signalling and tumorigenesis. *Nature* **2014**, *509*, 492–496. [CrossRef] [PubMed]

38. Liu, H.; Guo, H.; Jian, Z.; Cui, H.; Fang, J.; Zuo, Z.; Deng, J.; Li, Y.; Wang, X.; Zhao, L. Copper Induces Oxidative Stress and Apoptosis in the Mouse Liver. *Oxid. Med. Cell. Longev.* **2020**, *2020*, 1359164. [CrossRef] [PubMed]
39. Zhang, X.; Su, Y.; Yang, W.; Song, Z.; Sun, Z.; Wu, X.; Chen, J.; Gao, B.; Wang, Z.; Wang, L.; et al. Disruption of NF-κB-Mediated Copper Homeostasis Sensitizes Breast Cancer to Cuproptosis. *Adv. Sci.* **2025**, *12*, e06201. [CrossRef] [PubMed]
40. Cai, J.; Xie, H.; Yan, Y.; Huang, Z.; Tang, P.; Cao, X.; Wang, Z.; Yang, C.; Wen, J.; Tan, M.; et al. A novel cuproptosis-related lncRNA signature predicts prognosis and therapeutic response in bladder cancer. *Front. Genet.* **2022**, *13*, 1082691. [CrossRef] [PubMed]
41. Gehwolf, R.; Schwemberger, B.; Jessen, M.; Korntner, S.; Wagner, A.; Lehner, C.; Weissenbacher, N.; Tempfer, H.; Traweger, A. Global Responses of Il-1β-Primed 3D Tendon Constructs to Treatment with Pulsed Electromagnetic Fields. *Cells* **2019**, *8*, 399. [CrossRef] [PubMed]
42. Jiang, L.; Liu, T.; Lyu, K.; Chen, Y.; Lu, J.; Wang, X.; Long, L.; Li, S. Inflammation-related signaling pathways in tendinopathy. *Open Life Sci.* **2023**, *18*, 20220729. [CrossRef] [PubMed]
43. Nong, J.; Lu, G.; Huang, Y.; Liu, J.; Chen, L.; Pan, H.; Xiong, B. Identification of cuproptosis-related subtypes, characterization of immune microenvironment infiltration, and development of a prognosis model for osteoarthritis. *Front. Immunol.* **2023**, *14*, 1178794. [CrossRef] [PubMed]
44. Wu, Z.; Huang, Z.; Zhou, X.; Gao, C.; Peng, Z.; Zheng, X.; Zhang, Y.; Du, Z.; Wu, B. Comprehensive analysis of cuproptosis genes and cuproptosis-related genes as prognosis factors in esophageal squamous cell carcinoma. *Genomics* **2023**, *115*, 110732. [CrossRef] [PubMed]
45. Yang, W.; Xiao, C.; Zheng, J.; Song, J.; Li, X.-G. Copper homeostasis and cuproptosis represent emerging targets for therapeutic intervention in inflammatory diseases. *Pharmacol. Res.* **2025**, *221*, 107988. [CrossRef] [PubMed]
46. Ackerman, J.E.; Best, K.T.; Muscat, S.N.; Loiselle, A.E. Metabolic Regulation of Tendon Inflammation and Healing Following Injury. *Curr. Rheumatol. Rep.* **2021**, *23*, 15. [CrossRef] [PubMed]
47. Solmonson, A.; DeBerardinis, R.J. Lipoic acid metabolism and mitochondrial redox regulation. *J. Biol. Chem.* **2018**, *293*, 7522–7530. [CrossRef] [PubMed]
48. Zhang, L.; Deng, R.; Liu, L.; Du, H.; Tang, D. Novel insights into cuproptosis inducers and inhibitors. *Front. Mol. Biosci.* **2024**, *11*, 1477971. [CrossRef] [PubMed]
49. Xue, Q.; Kang, R.; Klionsky, D.J.; Tang, D.; Liu, J.; Chen, X. Copper metabolism in cell death and autophagy. *Autophagy* **2023**, *19*, 2175–2195. [CrossRef] [PubMed]

Disclaimer/Publisher's Note: The statements, opinions and data contained in all publications are solely those of the individual author(s) and contributor(s) and not of MDPI and/or the editor(s). MDPI and/or the editor(s) disclaim responsibility for any injury to people or property resulting from any ideas, methods, instructions or products referred to in the content.